HHS Public Access

Author manuscript

*Ear Hear*. Author manuscript; available in PMC 2019 July 01.

Published in final edited form as:

*Ear Hear*. 2018 ; 39(4): 712–719. doi:10.1097/AUD.0000000000000529.

# Theoretical evaluation and experimental validation of localized therapeutic hypothermia application to preserve residual hearing following cochlear implantation

**Ilmar Tamames**[1], **Curtis King**[2], **Chun Yuh Huang**[1], **Fred Telischi**[3], **Michael Hoffer**[3], and **Suhrud M. Rajguru**[1,3,*]

[1]Department of Biomedical Engineering, University of Miami, Miami, FL 33136

[2]Lucent Medical Systems, Seattle, WA

[3]Department of Otolaryngology, University of Miami, Miami, FL 33136

## Abstract

**Objectives—**Cochlear implantation surgery has been shown to result in trauma to inner ear sensory structures resulting in loss of residual hearing. Localized therapeutic hypothermia has been shown in clinical care to be a neuroprotective intervention. Previously we have shown in an experimental model that localized hypothermia protects cochlear hair cells and residual hearing function against surgical and cochlear implantation trauma. Using experimental temperature measurements carried out in human cadaver temporal bones and a finite element model of the inner ear, the present study examined the temperature distribution of a custom-designed hypothermia delivery system in the human inner ear organs.

**Design—**The efficacy of the hypothermia probe and resulting heat distribution across human cochlea and surrounding tissues were modeled in 3D in COMSOL. The geometry and dimensions of inner ear and temporal bones were derived from CT and MRI images. Model predictions were compared with experimental observations from five human temporal bones.

**Results—**In both the modeling and experimental studies, the cochlear temperature was lowered by 4–6 °C on the round window from a baseline of 37 °C within 16–18 minutes. The model simulations showed uniformly-distributed cooling across the cochlea. This study provides insight for design, operation and protocols for efficacious delivery of mild therapeutic hypothermia to the human cochlea that may significantly benefit patients undergoing surgical cochlear implantation by preserving residual hearing.

**Conclusion—**There was a close correlation between the results of the numerical simulations and experimental observations in this study. Our custom-designed system is capable of effectively providing mild therapeutic hypothermia locally to the human cochlea. When combined with

*Corresponding Author: Suhrud M. Rajguru, PhD, University of Miami Ear Institute: Sensory Electrophysiology Laboratory, 1600 NW 10th Ave, RMSB 3158, Miami, FL 33136. s.rajguru@miami.edu, Phone: 305-284-5434.

**Author contributions**

SMR and IT designed the study, SMR, IT and CH developed the model and carried out simulation study, SMR, IT, MH, and FT developed the temporal bone study and carried out experimental measurements, SMR, IT and CK developed and designed the hypothermia system used in this study, SMR and IT analyzed the results and prepared figures and manuscript, SMR, IT, CK, CH, MH and FT contributed to the final version of manuscript.

results from in vivo animal experiments, the present study suggests that the application of localized therapeutic hypothermia may hold potential for patients with an aim to preserve residual hearing after cochlear implantation.

**Keywords**

Therapeutic hypothermia; cochlear implant; residual hearing; auditory; deafness; trauma; neuroprotection

## 1. Introduction

More than 450,000 partially or completely deaf individuals have already received cochlear implantations worldwide (Cochlear 2016; FDA 2015). With the success of these devices and recent advances in technology, the indications for implantation have broadened to include patients with single-sided deafness, and those with loss of hearing at high frequencies and residual hearing at lower frequencies. Implantation of new hybrid (acoustic and electric) devices aims to take advantage of the remaining hair cells to allow for a wider range of acoustic representation, and may improve child development and quality of life for the patients (Markman et al. 2011). In particular, preservation of residual hearing during implantation may greatly aid early language development and the later development of speech perception skills in congenital and pre-lingual deaf children (Nikolopoulos et al. 1999; Tobey et al. 2013). However, cochlear implantation surgery has been shown to result in trauma to inner ear structures such as basilar membrane, osseous spiral lamina, and modiolus or by cascading molecular effects such as inflammation and oxidative stress (Bas et al. 2012; Eshraghi et al. 2005; Rebscher et al. 2008; Wardrop et al. 2005). In a recent clinical trial for an electric-acoustic stimulation (EAS) cochlear implant system, the most prevalent and significant adverse event was the loss of residual hearing (44% of the study population) (FDA 2013). Therefore, reducing the trauma caused by implantation and preservation of residual hearing remains an important research topic in the field. Further, a reduction of intra-cochlear damage caused during surgery may also limit fibrosis and ossification, which may be critical in cases where re-implantation may be required.

Localized mild therapeutic hypothermia has been a widely studied method for neuro-protection against secondary injuries as a result of brain trauma, strokes, spinal cord injuries and inner ear (Cappuccino et al. 2010; Dietrich et al. 2009; Dietrich et al. 2010; Dietrich et al. 2011; Eshraghi AA et al. 2007; Kawai et al. 2000; Levi et al. 2010). Modifying the temperature of the cochlea has been shown to influence auditory-evoked responses (Brown et al. 1983; Liberman et al. 1984; Ohlemiller et al. 1992, 1994), predominantly when applying hypothermia (Henry et al. 1984; Watanabe et al. 2001). While hyperthemia has been observed to lead to significantly elevated thresholds from noise-induced trauma compared to normothermic cochleae, hypothermia has been shown to have protective effects (Henry 2003). The beneficial effects of hypothermia have also been studied in an animal model of transient cochlear ischemia (Hyodo et al. 2001; Takeda et al. 2008). Hypothermia-treated cochleae, with a temperature of 32°C, were shown to have an improved recovery following ischemia injury along with a significant reduction in perilymphatic glutamate concentrations when compared to normothermic cochleae. Several studies, including our

group, have shown that animals undergoing surgical cochlear implantation and receiving hypothermia exhibited significantly less functional loss compared to normothermic implanted animals (Balkany et al. 2005; Eshraghi AA et al. 2007; Smith et al. 2007; Tamames et al. 2016). To aid clinical translation, we have designed and implemented a custom device to deliver localized hypothermia in a rodent model without requiring significant addition to the surgical duration (Tamames et al. 2016). Our results demonstrated that therapeutic hypothermia (a cooling of 4 to 6 °C from baseline (~37°C) measured at round window) applied during cochlear implantation preserves hair cells and residual hearing function and mitigates the adverse effects caused by surgical trauma. The hearing thresholds in implanted cochleae recovered to the pre-surgical levels matching the contralateral, control cochleae and remained steady up to 28 days post-implantation. The results from preclinical studies suggest a strong translational potential, especially for hypothermia delivered pre-trauma locally to the inner ear.

To assess the therapeutic efficacy of mild hypothermia while avoiding adverse effects and challenges of systemic cooling, it is critical to determine the feasibility of locally and controllably reducing the temperature at target structures. However, direct monitoring temperature of the inner ear without causing additional tissue damage is challenging in an animal model and not feasible in a clinical setting. To observe the spatial and temporal distribution of temperature within tissue surrounding the cochlear implant during the cooling procedure without requiring invasive techniques, we have developed a computational model that simulates temperature distribution in the inner ear. The experimentally validated model is designed to incorporate physical, geometrical, and physiological parameters under normal conditions in a three-dimensional geometry of inner ear and can be utilized to estimate efficacious cooling protocols to provide beneficial therapeutic hypothermia while avoiding damaging the inner ear structures. Such a model will be of significant value to the clinical and scientific community, and contribute to improving translational potential of therapeutic hypothermia for cochlear implant and other inner ear surgeries.

## 2. Methods

### 2.1 Theoretical model of the inner ear and hypothermia application

For the theoretical model, we utilized a simplified 3D reconstruction of temporal bone obtained from CT scans. The images and model were obtained from the University Health Network in Toronto by Dr. Eitan Aziza and provided for this study under Creative Commons license (https://skfb.ly/OVzX). The model mesh elements were reduced to 1k using MeshLab (Cignoni et al. 2008) to improve computational efficiency and imported in COMSOL (Comsol Inc., Burlington, MA). The 3D model of human inner ear (cochlea and vestibular endorgans) derived from MRI images from McGill University was simplified and provided by Dr. Seth Horowitz (http://www.thingiverse.com/thing:27340) under Creative Commons – Attribution – Share Alike license for this study. For the computational purposes, we reduced the mesh elements of the 3D human inner ear to 3k prior to importing it to COMSOL. The original and reduced models for the temporal bone and human inner ear are shown in Figure 1.

We utilized a finite element model created using a commercially available software package COMSOL (Comsol Inc., Burlington, MA). Finite element models of biological structures allow us to understand and predict biological phenomena and have been widely used in biomedical research over the past several decades (Ateshian et al. 2015; Jackson et al. 2011; Park et al. 2001; Petrov et al. 2017). Figure 2 shows the processed 3D images of the human temporal bone and inner ear organs imported into the numerical analysis tool. The 3D models were sized to scale and merged into a COMSOL mesh. For the present study, brain, skin or muscle tissue were not included since the primary focus was on the inner ear. However, the model can be easily extended in the future to use different values of surface heat transfer coefficient, tissue metabolic heat generation and physical, geometrical, and physiological parameters under normal conditions in a three-dimensional geometry of the head composed of the grey and white matters, the CSF layer, bone, the scalp and the muscle tissue. The temporal bone model size used in this study was ~90 mm in width and 70 mm in height. Inner ear organ model size was 6.2 mm in diameter for the cochlea and 7.1 mm in diameter for the superior semi-circular canal. The hypothermia probe cylindrical tip was similar to that used in previous animal and cadaver model studies at 1.6 mm in diameter and 5 mm in length. The values for the inner ear were set based on size assessments in literature (Erixon et al. 2009; Klopp-Dutote et al. 2016). The inner ear fluids were modeled as water for simplicity. The cylindrical hypothermia probe was positioned touching the cochlear bone, approximately 2.5 mm from the round window location. This orientation mimicked the position achievable under facial recess approach and that used for temporal bone temperature experiments (see below section 2.2).

We modeled a modified bio-heat equation, convection through bone and blood flow, metabolic heat generation and cooling provided by the hypothermia probe to the inner ear organs and temporal bone in COMSOL. A modified bio-heat equation utilizing the Pennes' approximation was used to describe the changes when mild hypothermia was applied at the probe. The bio-heat equation (equation 1) was adapted using the bio-heat transfer application mode with time dependency in COMSOL.

$$\rho_m C_m \, \partial T / \partial t + \nabla \cdot \left(-k_m \, \nabla \mathrm{T}\right) = \mathrm{Q} + \mathrm{Q}_{\mathrm{bio}} \quad (1)$$

Where T is the temperature; $\rho_m$, $C_m$ and $k_m$, are respectively the density, heat capacity and the thermal conductivity of the material for bone or water. Q is the boundary heat source coefficient of the hypothermia probe. Finally, $Q_{bio}$ is the blood metabolic heat source, derived using the equation:

$$\mathrm{Q}_{\mathrm{bio}} = \rho_{\mathrm{b}} \mathrm{C}_{\mathrm{b}} \omega_{\mathrm{b}} \left(\mathrm{T}_{\mathrm{b}} - \mathrm{T}\right) + \mathrm{Q}_{\mathrm{met}} \quad (2)$$

Where $\rho_b$ is the density for blood, $C_b$ is the specific heat capacity, $\omega_b$ is the perfusion rate, $T_b$ is the arterial temperature, T is temperature of the surrounding tissue and $Q_{met}$ is the metabolic heat source. These properties are listed in Table 1. It is assumed that the perfusion is homogeneous and isotropic. The tissues of interest were also assumed to be homogeneous

and isotropic. The material properties used in the present study were selected based on literature (Zhang et al. 2015) and default properties provided in COMSOL.

The bone, inner ear and cylindrical probe baseline temperature were initially set at 37°C. The temporal bone surface mesh, surrounding the sites of mastoid measurement and surgical opening was set to be influenced by room temperature (25°C). The remaining surface area, in particular the boundary open to the brain, was considered an open boundary with temperature set at 37 °C.

Of the three ways of heat transfer in a material, i.e. radiation, convection and conduction, we discounted both radiation and convection. The power radiated through the tissue is given by: $eb = \sigma\left(T_1^4 - T_2^4\right)$ where σ is the Stefan-Boltzmann constant (Lienhard 2013). So the net power radiated, from the probe cooled to ~20.2°C to the round window niche ~31.5°C, was estimated as $e_b \approx 68.5$ W/m$^2$. For comparison, the heat flux is a function of thermal conductivity and temperature gradient over distance: $q = -k\frac{dT}{dx}$ (Lienhard 2013). For a temperature difference of 11.3°C at a distance of 2.5 mm with a heat conduction of 0.32 W/m/°C, the heat flux density q is about 1450 W/m$^2$. Therefore, radiant heat transfer was neglected in our model in comparison with conduction.

For simplification in the present report, we did not model the fluid movement within the cochlea. The protocol for the therapeutic hypothermia followed previously reported experimental and *in vivo* animal studies (Tamames et al. 2016). In addition to the calculated temperature at the three sites (round window, oval window and mastoid), the heat distribution was calculated in modiolar and horizontal planes parallel to the probe starting at the round window and at every 1mm spanning the width and height of the cochlea.

### 2.2 Experimental measurements and validation using cadaver temporal bones

Experimental measurements were carried out using post mortem human temporal bones (n=5, k=8 trials) to mimic the surgical approach, probe location and protocols for therapeutic hypothermia application. The human cadaveric temporal bones were thawed overnight at room temperature to prepare them for surgical dissection. Once thawed sufficiently, the facial recess was approached by canal wall up mastoidectomy, a common surgical approach for cochlear implantation surgery. The boundaries of the facial recess i.e. the facial nerve, chorda tympani, and the incus buttress were identified. The round window and promontory were observed and recess expanded if deemed necessary. The bones were subsequently warmed to 37°C by submerging them in a water bath (Thermo Scientific Precision General Purpose Water Bath, model TSGP05) containing metallic beads (Lab Armor Beads, model 42370) set at 50 °C. To maintain the bone temperature during experimental measurements, they remained submerged in the bath. The hypothermia probe was placed anteroinferior to the round window via the facial recess. The custom device (Tamames et al. 2016) was used to apply cooling to the cochleae. A microthermistor (Omega, 5SC-TT-T-40-36) was placed on the surface of the mastoid to measure temperature changes over time. Two additional microthermistors were placed in the vicinity of the cochleae: one inserted via ear canal near the oval window and another one near the round window membrane via the facial recess approach.

The probe used to deliver localized mild hypothermia was connected to a custom thermoelectric Peltier system that circulated cooled or warmed fluorocarbon (Tamames et al. 2016). Fluorocarbons are chemically and thermally stable, with properties ideal for use as a heat transfer fluid and are generally non-toxic. The experimental protocol was based on our previous work, where the temperature of the circulating fluorocarbon, measured at the reservoir, was reduced in steps of 4°C every 2 minutes (starting temperature was set to 38°C, final fluorocarbon temperature achieved was 4°C). Note that this does not reflect the temperature at the probe due to losses along the length of catheter connecting reservoir to the probe end. Steady state temperature measurements were taken every two-minute step at the round window, oval window and mastoid surface using microthermistors.

### 2.3 Statistical analysis

Two-way ANOVA implemented in MATLAB (MathWorks, MA) was used to assess the changes in temperatures obtained from the experimental study. The comparison was made for measured temperatures at oval and round window locations on the cochleae against the control mastoid location. Values, that did not reach significance are represented with “ns”, values with $p < 0.05$ are represented by *, values with $p < 0.01$ are represented by ** and values with $p < 0.001$ are represented by ***.

## 3. Results

### 3.1 Numerical model of therapeutic hypothermia

Figure 4 shows a volumetric mesh of the temporal bone and inner ear used in the numerical analysis. The temperature contours showing heat distribution at the probe, across the inner ear and at the surface of the temporal bone at the final time point in cooling protocol are shown. The simulated cooling was calculated at three sites: round window, oval window and mastoid. The volume nearest to the probe reached temperatures near 30°C, while the cochlear temperature varied between 31°C at the round window and 33°C at the oval window. The surface of the temporal bone did not cool significantly in comparison.

Figure 5 shows temperature contours in 2D at six modiolar isothermal slices across the temporal bone including the cochlea, starting from the round window (A1, nearest to the probe) and traversing the cochlea every 1 mm (A2–A6). The bottom part of the contours representing the inside face of the temporal bone did not achieve significant cooling. However, the volume that includes the cochlea cooled between 31–33°C uniformly.

Figure 6 shows temperature contours in 2D at four horizontal isothermal slices across the temporal bone including the cochlea, starting from the basal turn and traversing the cochlea every 1 mm until the apical turn (A1–A4). The slices include the hypothermia probe and also show that the volume that includes the cochlea cooled between 31–33°C uniformly.

The specific temperatures during hypothermia protocol were calculated at the round window, oval window via ear canal approach and mastoid (Figure 7A). The set temperature for the hypothermia probe over the same duration is shown on the right vertical axis. Over a period of 18 minutes, the temperature drop was calculated to be ~6°C (starting temperature was selected at 37°C) at the round window. The temperature at the oval window was reduced

by ~3.5 °C from the baseline, while the mastoid temperature did not reduce significantly (0.5 °C). The calculated cooling results closely correlate with probe temperature, and reach levels that will be required for in vivo application.

### 3.2 Experimental validation in cadaver temporal bones

Temperature measurements were carried out in 5 cadaver temporal bones over 8 trials to analyze the translational potential of this device. The locations of microthermistors, the orientation of the probe and facial recess are identified in Figure 3. Figure 7B,C show the measured temperatures at the round window, oval window and mastoid surface. The temporal bones were warmed in a bath to achieve a baseline between 36 to 38°C in the cochleae and approximately 35°C at the mastoid surface. The mastoid surface was affected only by the room temperature and as a result, its temperature did not reduce significantly (~1°C). The mean starting temperature at the round window was ~1.4 ± 0.16 °C higher than that observed at the oval window (8 trials). The difference was due to positioning of the cadaver bone within the bath and placement of thermistors at individual sites. During experimental setup, the boundaries of the facial recess were recognized: the facial nerve, chorda tympani, and the incus buttress. The round window and promontory were observed and the probe was placed superior to the round window. This close proximity provided higher cooling (~1°C) at the round window compared to oval window. Overall, with the present system and placement of the hypothermia probe through the facial recess, the temperature at the round window reduced by an average of 5.41 °C following a hypothermia protocol lasting 18 minutes. The temperature at the oval window was observed to reduce by an average of 4.36 °C from baseline with the hypothermia treatment. The total change in temperature at the cochlear round and oval window locations over baseline temperature measured prior to hypothermia treatment was significant when compared to the change measured at the mastoid location (Figure 7C, inset, $p<0.001$).

## 4. Discussion

The distribution of temperatures across an anatomically accurate 3D human cochlear geometry in response to the placement of hypothermia delivery system near the round window niche was investigated as a function of anatomical location and compared with experimental observations in a cadaveric temporal bone. We built upon previous studies that utilized simplified models and experimental approaches to investigate translational potential of therapeutic hypothermia application. Similar approach was employed to simulate hypothermia treatments to lower the brain temperature and identified a neckband, covering the carotid triangles of the neck, as a successful technique (Keller et al. 2009). Theoretical and *in-vivo* experiments showed the effectiveness of a torso-cooling pad to reduce the temperature in the spinal cord and brain in rats (Smith 2011). Following these studies, we utilized Pennes bio-heat equation and finite element analysis to simulate the temperature distribution in the cochlea during therapeutic hypothermia. Studies of heat distribution in the cochlea during infrared stimulation utilized simplified geometries to effectively identify an increase of the cochlear temperature (De Paolis et al. 2017; Liljemalm et al. 2013; Manoussaki et al. 2000; Zhang et al. 2015). The present study produced a novel numerical analysis model that instead used true 3D inner ear organ and temporal bone geometries

derived from MRI and CT scans. The model calculations provide insight into the localized effects of the temperature distribution and allow visualization of temperature gradients in otherwise inaccessible locations. Our simulations show that the temperature at the round window reaches mild hypothermia (32–33 °C) in approximately 16–18 minutes from baseline levels. The temperature at the oval window reduced by 4°C, settling at ~33°C, the optimal level for mild therapeutic hypothermia during the cooling procedure. The detailed distribution profiles along modiolar and horizontal planes (Figures 5, 6) clearly show that the mild hypothermic treatment permeates from the basal turn volume closest to the probe to the apex region of the cochlea.

To work towards translating such a device for clinical therapeutic hypothermia treatment, the model results were validated experimentally. For this purpose, efficacy of the hypothermia device was tested in cadaver temporal bones. The experimental measurements showed similar temperate decrease and rate of change at the three locations compared: the round window, oval window and mastoid surface. Long-duration thermal equilibrium of the temporal bones (near 37°C) was achieved by immersing the bones in a heated metallic-bead bath. Utilizing the custom hypothermic device placed next to the round window niche via the facial recess, we succeeded in reducing the temperature at the round window to 32–33 °C (by 6°C on average) within an 18 minutes cooling period. In comparison, the temperature at the oval window reduced to 32°C (by 4°C on average) and the mastoid surface temperature remained unchanged, affected mostly by room temperature. In a previous study, we demonstrated the hypothermia application as a tool in otoprotection and established that functional capacity of the cochlea was restored in an animal model (Tamames et al. 2016). Results showed that the hearing thresholds in hypothermic-treated and implanted cochleae recovered to the pre-surgical levels. Histological results demonstrated survival of hypothermia-treated outer hair cells as compared to untreated outer hair cells. The current results combined with this previous study, suggest that using our approach for a localized therapeutic hypothermia treatment may be successfully provided to the human inner ear during cochlear implantation and other neurotologic surgeries.

Several limitations need consideration and further study prior to transferring the results of the model and temperature recordings into a clinical application. While performing the experiments, we identified that the facial recess may need minor modification for placement of the probe. In several of the bones it was possible to create a small facial recess and to place the hypothermia probe while simultaneously visualizing the round window. In clinical practice, it may be preferable to open the facial recess more widely to improve visualization of the round window niche, and to better allow for optimal placement of the probe. This may also facilitate creation of a cochleostomy for insertion of the electrode array, if necessary. An alternative approach for the placement of probe may be through a myringotomy, which will be explored in a future study. Experimental observations and simulations suggest that 16–18 minutes may be necessary to achieve the optimal temperature required for mild therapeutic hypothermia. In comparison the *in vivo* rat model cooling period was shorter in the previous study (Tamames et al. 2016) and may need to be reduced for the clinical application. There are several factors that may explain the longer durations required in the current application. In the present study, we did not model the movement of the inner ear fluids or blood perfusion within the cochlea. Several studies have confirmed the presence of local and

temporal pressure gradients that may be important factors contributing to heat transfer (De Paolis et al. 2017; Olson 1999; Salt et al. 2001; Salt et al. 1986). The present model also does not take into account differences in soft and hard tissues in the human ear and may benefit from higher resolution, micro-computer tomography (CT) geometric model (De Paolis et al. 2017; Manoussaki and Chadwick 2000). Finally, based upon our previously published experiments in the rat model of cochlear implantation (Tamames et al. 2016), we developed the hypothermia protocol to incorporate rewarming the cochleae to baseline temperature. This recovery to 37°C is managed using the same probe and system. In the present report, we did not explicitly measure the rewarming as the primary focus was to study the efficacy of cooling. A rigorous analysis of speed of rewarming will be necessary to optimize the hypothermia protocol for application in the operating room.

## 5. Conclusion

Overall, there is a close correlation between the results of the numerical simulations and experimental observations in this study. Our custom-designed hypothermia system is capable of effectively providing mild therapeutic hypothermia locally to the human cochlea. When combined with results from in vivo animal experiments, the present study suggests that the application of localized therapeutic hypothermia may hold potential for patients with an aim to preserve residual hearing after cochlear implantation.

## Acknowledgments

Funding for this study was provided by NIDCD R21DC014324, NIDCD R01DC013798 and Cochlear to SMR. The authors sincerely thank Dr. Thomas Babcock and Ms. Jennifer Pineros for their technical help during the study.

**Conflict of interest and source of funding**

SMR and MH are funded by Cochlear to develop the therapeutic hypothermia application for cochlear implant surgery. SMR and CK are named inventors on a patent for the hypothermia system used in this study. Funding for this study was provided by NIDCD R21DC014324, NIDCD R01DC013798 and Cochlear to SMR.

## References

Ateshian GA, Henak CR, Weiss JA. Toward patient-specific articular contact mechanics. J Biomech. 2015; 48:779–786. [PubMed: 25698236]

Balkany TJ, Eshraghi AA, Jiao H, et al. Mild hypothermia protects auditory function during cochlear implant surgery. Laryngoscope. 2005; 115:1543–1547. [PubMed: 16148692]

Bas E, Dinh CT, Garnham C, et al. Conservation of hearing and protection of hair cells in cochlear implant patients' with residual hearing. Anat Rec (Hoboken). 2012; 295:1909–1927. [PubMed: 23044907]

Brown MC, Smith DI, Nuttall AL. The temperature dependency of neural and hair cell responses evoked by high frequencies. J Acoust Soc Am. 1983; 73:1662–1670. [PubMed: 6863743]

Cappuccino A, Bisson LJ, Carpenter B, et al. The use of systemic hypothermia for the treatment of an acute cervical spinal cord injury in a professional football player. Spine (Phila Pa 1976). 2010; 35:E57–62. [PubMed: 20081503]

Cignoni P, Callieri M, Corsini M, et al. Meshlab: an open-source mesh processing tool. Eurographics Italian Chapter Conference. 2008:129–136.

2016 Cochlear Annual Report [database online]. Cochlear. 2016

De Paolis A, Watanabe H, Nelson JT, et al. Human cochlear hydrodynamics: A high-resolution μCT-based finite element study. Journal of Biomechanics. 2017; 50:209–216. [PubMed: 27855986]

Dietrich WD, Atkins CM, Bramlett HM. Protection in animal models of brain and spinal cord injury with mild to moderate hypothermia. J Neurotrauma. 2009; 26:301–312. [PubMed: 19245308]

Dietrich WD, Bramlett HM. The evidence for hypothermia as a neuroprotectant in traumatic brain injury. Neurotherapeutics. 2010; 7:43–50. [PubMed: 20129496]

Dietrich WD, Levi AD, Wang M, et al. Hypothermic treatment for acute spinal cord injury. Neurotherapeutics. 2011; 8:229–239. [PubMed: 21416406]

Erixon E, Hogstorp H, Wadin K, et al. Variational anatomy of the human cochlea: implications for cochlear implantation. Otol Neurotol. 2009; 30:14–22. [PubMed: 18833017]

Eshraghi AA, Adil E, He J, et al. Local Dexamethasone Therapy Conserves Hearing in an Animal Model of Electrode Insertion Trauma-Induced Hearing Loss. Otology & Neurotology. 2007; 28:842–849. [PubMed: 17471110]

Eshraghi AA, Polak M, He J, et al. Pattern of hearing loss in a rat model of cochlear implantation trauma. Otol Neurotol. 2005; 26:442–447. [PubMed: 15891647]

FDA. Executive Summary, Cochlear Corporation Nucleus Hybrid L24 System Premarket Approval P130016. 2013

FDA. FDA executive summary: premarket to postmarket shifts in clinical data requirements for cochlear implant device approvals in pediatric patients. Ear, Nose, and Throat Devices Panel of the Medical Devices Advisory Committee; 2015. http://www.fda.gov/downloads/AdvisoryCommittees/CommitteesMeetingMaterials/MedicalDevices/MedicalDevicesAdvisoryCommittee/EarNoseandThroatDevicesPanel/UCM443996.pdf

Henry KR. Hyperthermia exacerbates and hypothermia protects from noise-induced threshold elevation of the cochlear nerve envelope response in the C57BL/6J mouse. Hearing Research. 2003; 179:88–96. [PubMed: 12742241]

Henry KR, Chole RA. Hypothermia protects the cochlea from noise damage. Hear Res. 1984; 16:225–230. [PubMed: 6401081]

Hyodo J, Hakuba N, Koga K, et al. Hypothermia reduces glutamate efflux in perilymph following transient cochlear ischemia. Neuroreport. 2001; 12:1983–1987. [PubMed: 11435934]

Jackson AR, Huang CY, Brown MD, et al. 3D finite element analysis of nutrient distributions and cell viability in the intervertebral disc: effects of deformation and degeneration. J Biomech Eng. 2011; 133:091006. [PubMed: 22010741]

Kawai N, Okauchi M, Morisaki K, et al. Effects of delayed intraischemic and postischemic hypothermia on a focal model of transient cerebral ischemia in rats. Stroke. 2000; 31:1982–1989. discussion 1989. [PubMed: 10926967]

Keller E, Mudra R, Gugl C, et al. Theoretical evaluations of therapeutic systemic and local cerebral hypothermia. J Neurosci Methods. 2009; 178:345–349. [PubMed: 19167429]

Klopp-Dutote N, Kolski C, Biet A, et al. A radiologic and anatomic study of the superior semicircular canal. Eur Ann Otorhinolaryngol Head Neck Dis. 2016; 133:91–94. [PubMed: 26671715]

Levi AD, Casella G, Green BA, et al. Clinical outcomes using modest intravascular hypothermia after acute cervical spinal cord injury. Neurosurgery. 2010; 66:670–677. [PubMed: 20190669]

Liberman MC, Dodds LW. Single-neuron labeling and chronic cochlear pathology. II. Stereocilia damage and alterations of spontaneous discharge rates. Hear Res. 1984; 16:43–53. [PubMed: 6511672]

Lienhard, JH. A heat transfer textbook. Courier Corporation; 2013.

Liljemalm R, Nyberg T, von Holst H. Heating during infrared neural stimulation. Lasers Surg Med. 2013; 45:469–481. [PubMed: 23832680]

Manoussaki D, Chadwick RS. Effects of geometry on fluid loading in a coiled cochlea. SIAM Journal on Applied Mathematics. 2000; 61:369–386.

Markman TM, Quittner AL, Eisenberg LS, et al. Language development after cochlear implantation: an epigenetic model. Journal of Neurodevelopmental Disorders. 2011; 3:388–404. [PubMed: 22101809]

Nikolopoulos TP, O'Donoghue GM, Archbold S. Age at implantation: its importance in pediatric cochlear implantation. Laryngoscope. 1999; 109:595–599. [PubMed: 10201747]

Ohlemiller KK, Siegel JH. The effects of moderate cooling on gross cochlear potentials in the gerbil: basal and apical differences. Hear Res. 1992; 63:79–89. [PubMed: 1464578]

Ohlemiller KK, Siegel JH. Cochlear basal and apical differences reflected in the effects of cooling on responses of single auditory nerve fibers. Hear Res. 1994; 80:174–190. [PubMed: 7896576]

Olson ES. Direct measurement of intra-cochlear pressure waves. Nature. 1999; 402:526–529. [PubMed: 10591211]

Park HK, Dujovny M, Park T, et al. Application of finite element analysis in neurosurgery. Childs Nerv Syst. 2001; 17:87–96. [PubMed: 11219630]

Petrov PI, Mandija S, Sommer IEC, et al. How much detail is needed in modeling a transcranial magnetic stimulation figure-8 coil: Measurements and brain simulations. PLoS One. 2017; 12:e0178952. [PubMed: 28640923]

Rebscher SJ, Hetherington A, Bonham B, et al. Considerations for the design of future cochlear implant electrode arrays: Electrode array stiffness, size and depth of insertion. Journal of rehabilitation research and development. 2008; 45:731–748. [PubMed: 18816423]

Salt AN, Ma Y. Quantification of solute entry into cochlear perilymph through the round window membrane. Hear Res. 2001; 154:88–97. [PubMed: 11423219]

Salt AN, Thalmann R, Marcus DC, et al. Direct measurement of longitudinal endolymph flow rate in the guinea pig cochlea. Hear Res. 1986; 23:141–151. [PubMed: 3745017]

Smith KD. Experimental study and model validation of selective spinal cord and brain hypothermia induced by a simple torso-cooling pad. Proc Inst Mech Eng H. 2011; 225:533–547. [PubMed: 22034738]

Smith LP, Eshraghi AA, Whitley DE, et al. Induction of localized cochlear hypothermia. Acta Otolaryngol. 2007; 127:228–233. [PubMed: 17364357]

Takeda S, Hakuba N, Yoshida T, et al. Postischemic mild hypothermia alleviates hearing loss because of transient ischemia. Neuroreport. 2008; 19:1325–1328. [PubMed: 18695517]

Tamames I, King C, Bas E, et al. A cool approach to reducing electrode-induced trauma: Localized therapeutic hypothermia conserves residual hearing in cochlear implantation. Hear Res. 2016; 339:32–39. [PubMed: 27260269]

Tobey EA, Thal D, Niparko JK, et al. Influence Of Implantation Age On School-Age Language Performance In Pediatric Cochlear Implant Users. International journal of audiology. 2013; 52:219–229. [PubMed: 23448124]

Wardrop P, Whinney D, Rebscher SJ, et al. A temporal bone study of insertion trauma and intracochlear position of cochlear implant electrodes. I: Comparison of Nucleus banded and Nucleus Contour electrodes. Hear Res. 2005; 203:54–67. [PubMed: 15855030]

Watanabe F, Koga K, Hakuba N, et al. Hypothermia prevents hearing loss and progressive hair cell loss after transient cochlear ischemia in gerbils. Neuroscience. 2001; 102:639–645. [PubMed: 11226700]

Zhang K, Ma Y, Zhou Y, et al. Effects of heat conduction on the spatial selectivity of infrared stimulation in the cochlea. Biomed Eng Online. 2015; 14:23. [PubMed: 25889277]

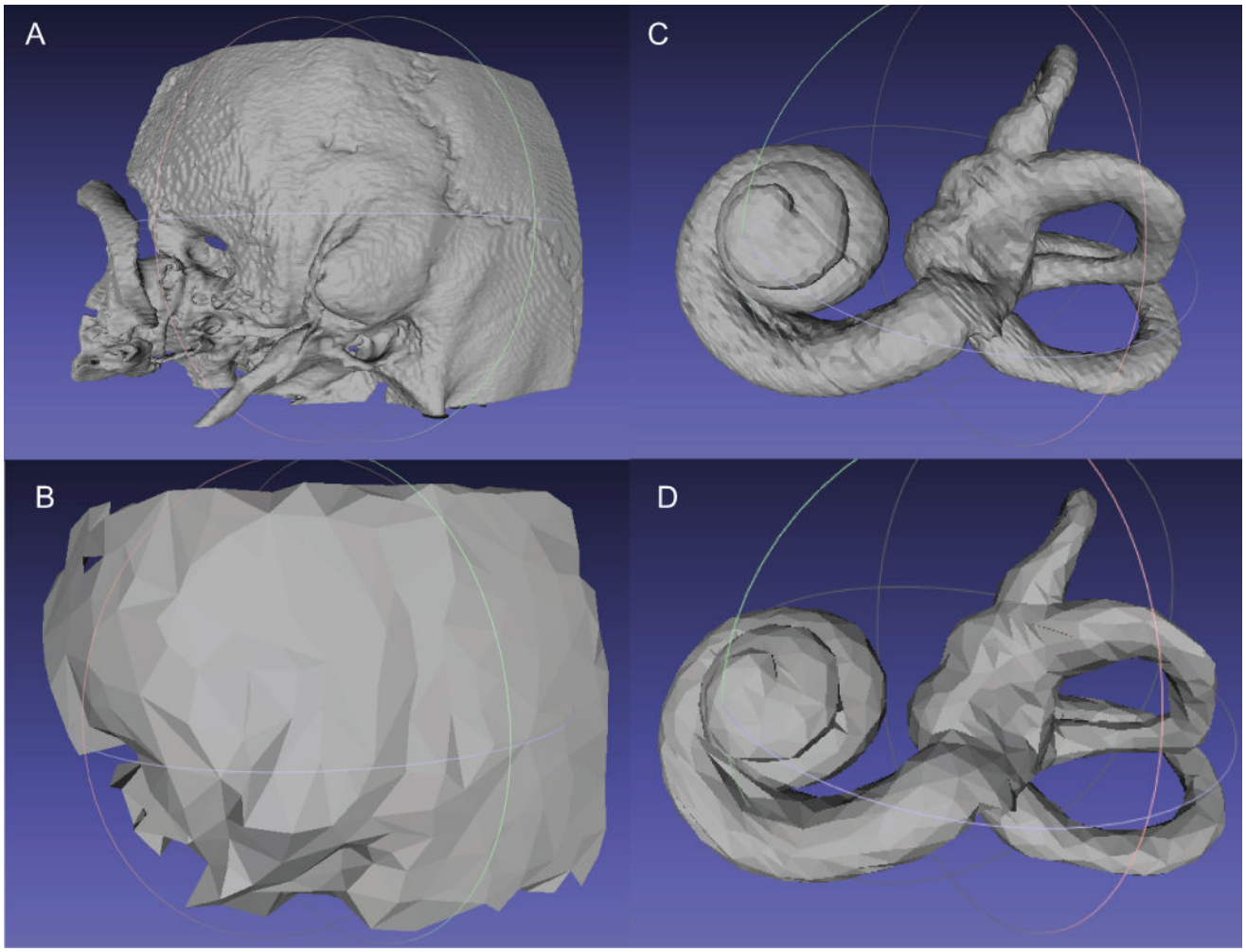


**Figure 1.**

The model setup used in this study. (A, C) show the images of temporal bone and inner ear organs re-constructed from CT and MRI scans. (B, D) show the simplified, reduced mesh versions of the same models prior to importing in COMSOL.

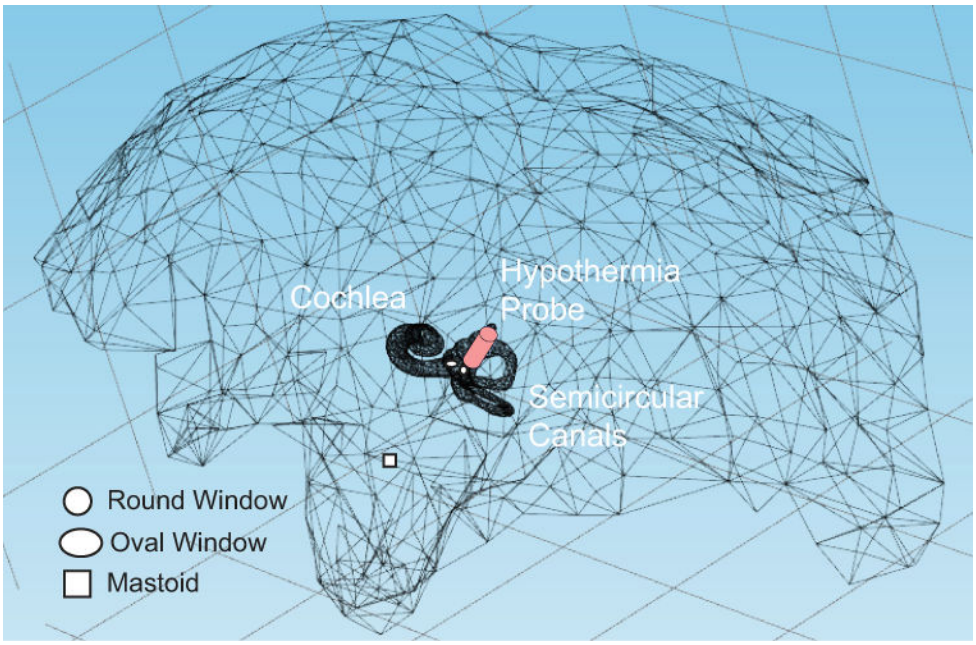


**Figure 2.**

The COMSOL model mesh setup. The simplified, reduced mesh including temporal bone and inner ear organs is shown along with the hypothermia probe mimicking potential surgical orientation contacting the round window niche. The locations of round window, oval window and mastoid are highlighted. Temperatures at these three locations, in addition to multiple planes along the inner ear were simulated.

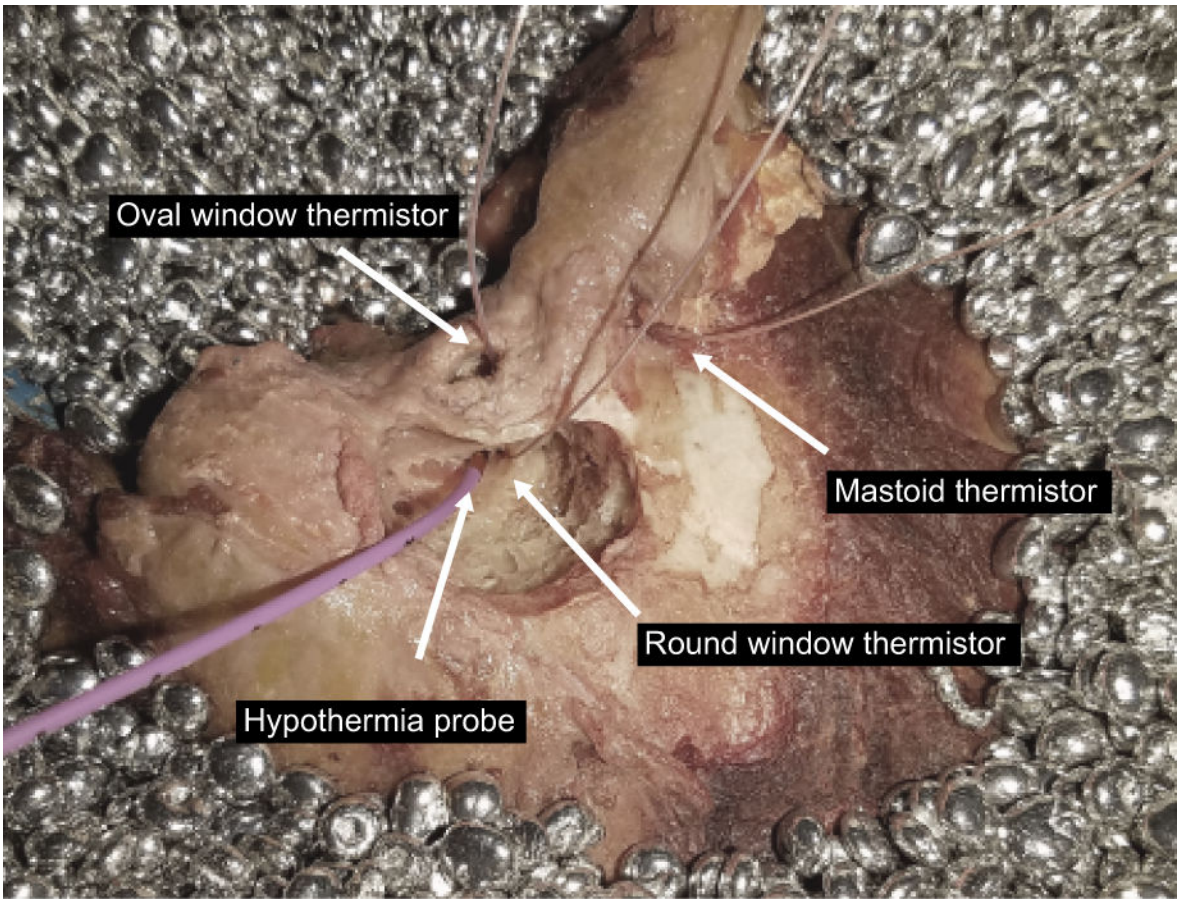


**Figure 3.**

Experimental setup for cadaver temporal bone measurements. Dissected human cadaveric temporal bones were prepared to study the effectiveness of the hypothermia probe. Bones were submerged in a metallic bead warm bath. A custom-designed hypothermia probe was placed anteroinferior to the round window via prepared facial recess approach. Three thermistors were placed at the sites of round window, oval window and mastoid surface.

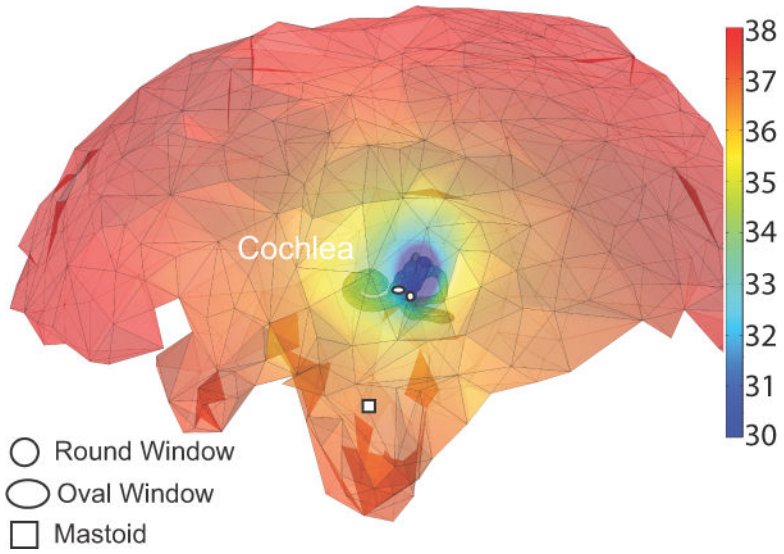


**Figure 4.**

The numerical 3D model of the temporal bone with the temperature distribution achieved from localized mild hypothermia. Locations of round window, oval window and mastoid thermistors are represented. Temperature contour was obtained at 18 minutes into the hypothermia protocol. The representative color scale was fixed between 30–38°C.

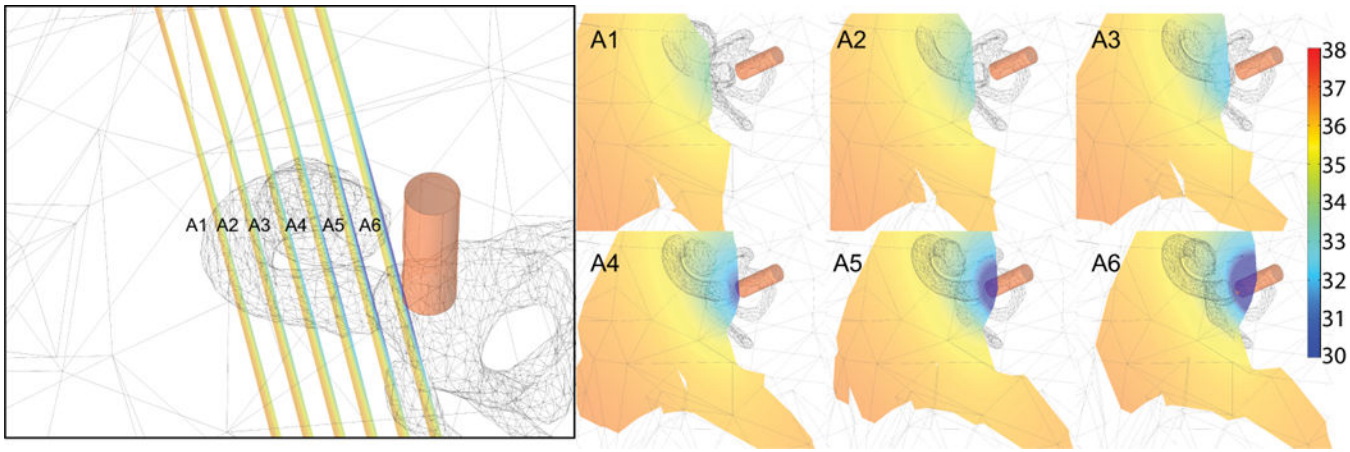


**Figure 5.**

The simulated temperature contours across the temporal bone and cochlea. The contour surfaces represent modiolar slices parallel to the probe every 1 mm. The inset shows the same surfaces rotated in the z-plane for ease of visualization. The color scale representing temperatures was fixed between 30–38°C.

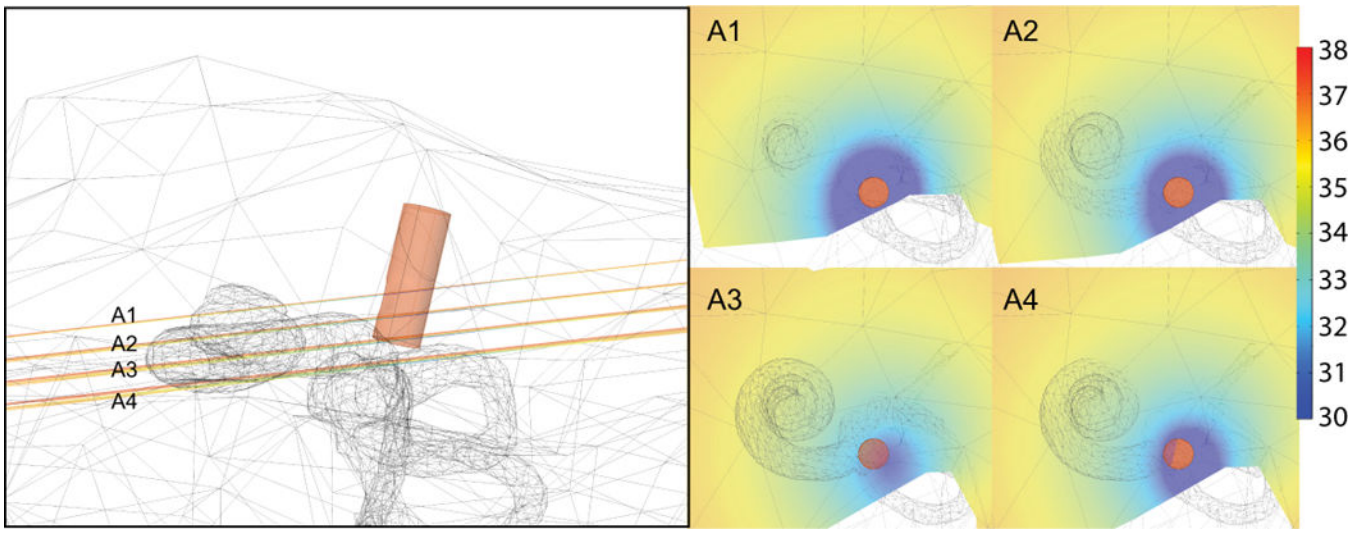


**Figure 6.**

The simulated temperature contours across the temporal bone and cochlea. The contours surfaces represent horizontal slices parallel traversing the cochlea every 1 mm. The inset shows the same surfaces in the x, y-plane for ease of visualization. The color scale representing temperatures was fixed between 30–38°C.

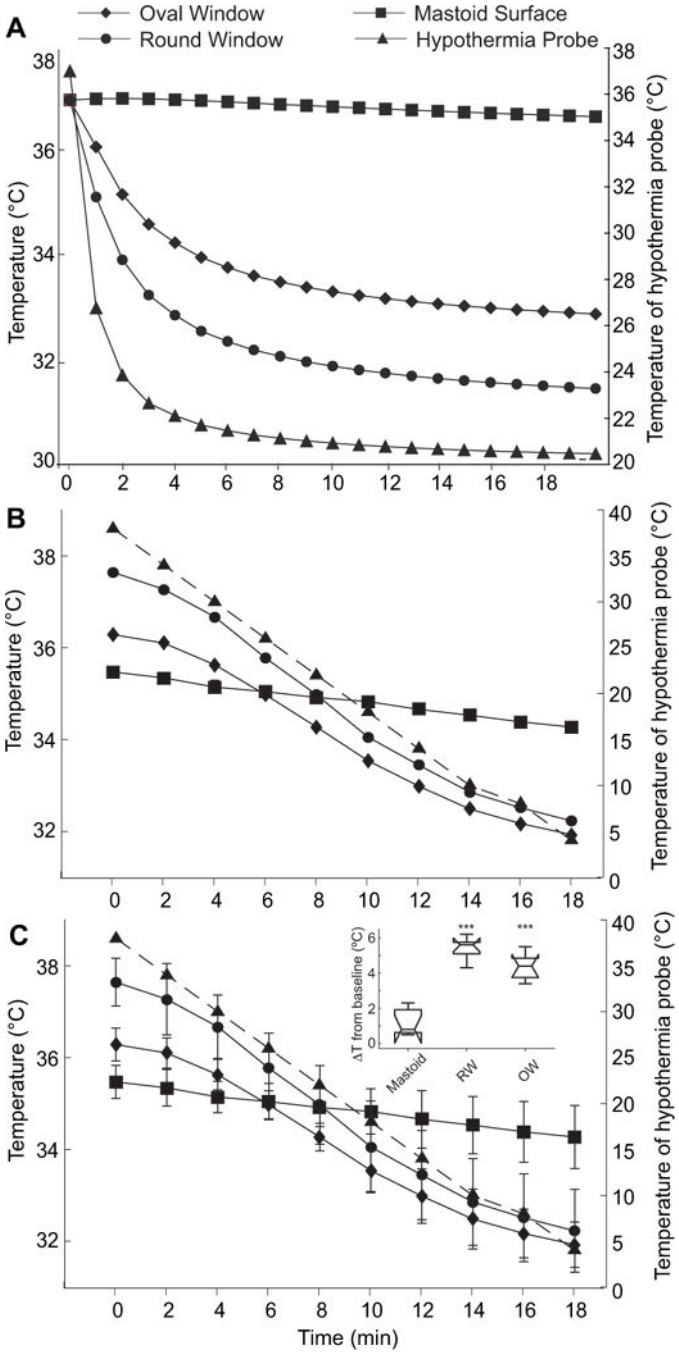


**Figure 7.**

The numerically and experimentally obtained temperatures at the round window, oval window and mastoid surface achieved with localized hypothermia probe. (A) shows the results from numerical simulation. With the hypothermia protocol, the temperatures across cochlea measured at round and oval windows reduced by an average of 4–6 °C while the surface of temporal bones remained near baseline. (B) shows the experimentally obtained temperature measurements taken from cadaveric temporal bones (mean from n=5, 8 trials). With the hypothermia protocol, a significant drop in temperature was observed at round and

oval windows. The cadaver temporal bones were warmed to achieve a baseline between 36–38°C. The mastoid temperature (filled triangles) did not change significantly (change of <1 °C). (C) shows the experimentally obtained temperature measurements (mean ± S.D.) taken from cadaveric temporal bones. Inset shows the total change over baseline at the three locations. *** $p < 0.001$

**Table 1**

Physiological properties used in model computations.

| Type | Density (kg/m$^3$) | Specific Heat Capacity (J/kg·K) | Thermal Conductivity (W/m·K) | Blood Perfusion Rate (1/s) | Metabolic Heat Generation (W/m$^3$) |
|---|---|---|---|---|---|
| Temporal Bone | *1,908* | *1313* | *0.32* | – | – |
| Perilymph/Endolymph (modeled as water) | *994* | *4178* | *0.60* | – | – |
| Blood | *1,050* | *3840* | *0.52* | *0.00033* | *1,100* |